MITSUBISHI ELECTRIC RESEARCH LABORATORIES
https://www.merl.com

Experimental Analysis of Mismatched Soft-Demapping for Probabilistic Shaping in Short-Reach Nonlinear Transmission

Skvortcov, Pavel; Millar, David S.; Phillips, Ian; Forysiak, Wladek; Koike-Akino, Toshiaki; Kojima, Keisuke; Parsons, Kieran

TR2021-109 September 16, 2021

Abstract

The impact of dimensionality of soft-demappers is investigated for probabilistic shaping in systems with short-memory correlated nonlinearities. Simple instantaneous nonlinearity compensation is proposed, significantly improving the performance of a low-complexity 1D demapper.

European Conference on Optical Communication (ECOC) 2021

Experimental Analysis of Mismatched Soft-Demapping for Probabilistic Shaping in Short-Reach Nonlinear Transmission

Pavel Skvortcov(1), David S. Millar(2,3), Ian Phillips(1), Wladek Forysiak(1), Toshiaki Koike-Akino(2), Keisuke Kojima(2), Kieran Parsons(2)

(1) Aston University, Birmingham, B4 7ET, UK. skvortcp@aston.ac.uk
(2) Mitsubishi Electric Research Laboratories (MERL), Cambridge, MA 02139, USA. koike@merl.com
(3) Infinera Corporation, San Jose, CA 95119, USA.

Abstract *The impact of dimensionality of soft-demappers is investigated for probabilistic shaping in systems with short-memory correlated nonlinearities. Simple instantaneous nonlinearity compensation is proposed, significantly improving the performance of a low-complexity 1D demapper.*

Introduction

Probabilistic shaping in combination with soft-decision (SD) forward error correction (FEC) has been considered as an important technology for high-capacity coherent fiber-optical communication systems, rapidly evolving from an early research proposal[1] to realizable[2] and commercial[3] technology. Probabilistic shaping can be integrated into bit-interleaved coded modulation (BICM) systems using the probabilistic amplitude shaping (PAS) framework[1]. This allows low implementation complexity, while offering additional gains via optimized signaling schemes for improved energy efficiency or nonlinear tolerance[4].

Recently, it was shown that practical finite-length probabilistic shaping can offer considerable nonlinear gain in addition to linear shaping gain[5],[6], especially, in short-memory fiber links subject to strongly correlated nonlinear noise[7]–[9]. In particular, the advantage of short-length shaping was demonstrated using Huffman-coded sphere shaping (HCSS) in extended-reach single-span links[8],[9]. The highest gain is observed for 4D symbol mapping, which results in a single shaped sequence being mapped onto all 4 quadratures of the signal concurrently, and therefore benefits from 4D soft-demapping at the receiver[10]. 4D demappers allow consideration of advanced noise statistics with correlation between dimensions, which may also provide performance gains in highly nonlinear links[11],[12].

In this work, we study the impact of the dimensionality of mismatched soft-demappers with advanced noise statistics on the achievable information rate (AIR) of probabilistically shaped signals. Transmission performance is characterized in an extended-reach single-span link, where the signal is impacted by strongly correlated nonlinearities and the optimal 4D shaped signal mapping is used. We then analyze the relative performance of instantaneous nonlinearity compensation on the low-complexity demappers.

Mismatched Soft-Demapping

In BICM systems, soft-demapping is used to calculate reliabilities of bits corresponding to the received symbols in the form of log-likelihood ratios (LLRs), which are then used for SD-FEC decoding to recover the transmitted information. Typically, the true channel is not known and soft-demapping is preformed based on simplified auxiliary channel assumptions, which we refer to as mismatched soft-demapping. The common choice for an auxiliary channel is the memoryless additive white Gaussian noise (AWGN) channel, modeled as[11]:

$$f_{Y|X}(y|x') = \frac{\exp(-\frac{1}{2}(y-x')^{\mathrm{T}}\boldsymbol{\Sigma}^{-1}(y-x'))}{\sqrt{(2\pi)^d|\boldsymbol{\Sigma}|}}, \quad (1)$$

where d is the dimensionality of the channel, $\boldsymbol{\Sigma}$ is a $d \times d$ covariance matrix ($|\boldsymbol{\Sigma}|$ is its determinant), y is the received symbol, and x' represents the centroid of the received symbols y corresponding to the transmitted symbol x. LLRs for binary labels B_i ($i = 1, \ldots, m$) of the received symbol are calculated by the soft-demapper as:

$$\mathrm{LLR}_i = \log \frac{\sum_{x \in \mathcal{X}_{1,i}} f_{Y|X}(y|x')P_X(x)}{\sum_{x \in \mathcal{X}_{0,i}} f_{Y|X}(y|x')P_X(x)}, \quad (2)$$

where $\mathcal{X}_{1,i}$ and $\mathcal{X}_{0,i}$ are the subsets of constellation $\mathcal{X}$ for B_i equal to 1 or 0, respectively; $P_X(x)$ is the probablity mass function (PMF).

An auxiliary channel allows various options for noise statistics calculations for soft-demapping,

978-1-6654-3868-1/21/$31.00 ©2021 IEEE

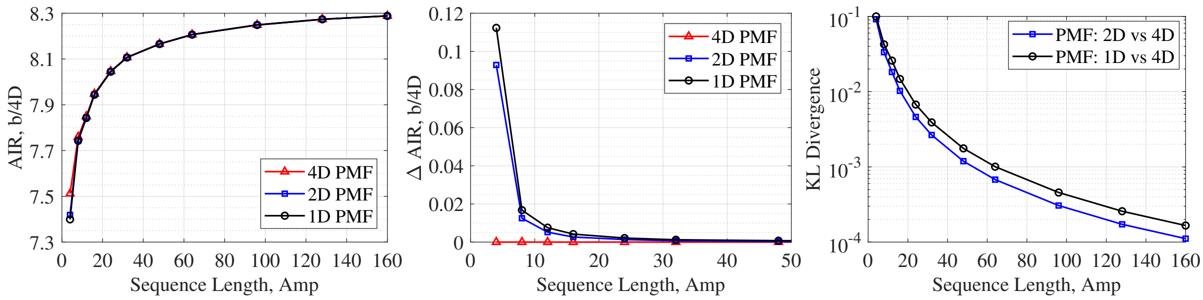

(a) AIR vs. shaping length **(b)** AIR penalty wrt. 4D PMF **(c)** KL divergence vs. shaping length

Fig. 1: Impact of soft-demappers with mismatched PMF.

Tab. 1: Soft-demappers

Parameter	Type	Description
Dimensionality	1D	1D aux. ch. & centroids
	2D	2D aux. ch. & centroids
	4D	4D aux. ch. & centroids
Noise statistics	CS	circularly symmetric
	VPD	variances per dimension
	CG	correlated Gaussian
Covariance type	AC	average covariance
	SC	symbol-wise covariance

the simplest of which is a circularly symmetric (CS) statistics, whereby the covariance matrix is the identity matrix multiplied by an average noise variance. Another option is to define noise variances per dimension (VPD) neglecting cross-correlations, in which case, the covariance matrix is diagonal with variances per dimension. An advanced approach is to calculate correlated Gaussian (CG) noise statistics where the full covariance matrix is defined. Furthermore, we distinguish two cases: when covariance matrices are defined per all constellation symbols (average covariance, AC) or per each symbol separately (symbol-wise covariances, SC). The soft-demapper parameters are summarized in Tab. 1.

Mismatched PMF: Soft-demapping requires that symbol likelihoods are conditioned on the probability distribution of the signal. When asymptotically large shaping sequences are used, it is valid to consider the different symbols comprising a sequence as independent and identically distributed. However, as the length of the shaping sequence is reduced, this approach becomes increasingly inaccurate. While the full calculation of symbol likelihoods for finite sequence lengths is conditioned on the symbol and all other symbols which comprise the sequence, this approach is computationally equivalent to maximum likelihood detection of shaped sequences, and negates the powerful advantages of the PAS architecture.

We examine the impact of using soft-demappers with mismatched PMFs for shaped signals in the AWGN channel by numerical simulation using HCSS[9] with shaping rate of 1.75 b/Amp and 4D symbol mapping based on DP-64QAM; and a signal-to-noise ratio (SNR) of 12.5 dB. Three soft-demappers are compared: 1D (where the 1D PMF is calculated using only the frequency of symbols in the entire set of shaping sequences), 2D and 4D (where PMFs are calculated using the frequency of pairs and 4-tuples of symbols in the set of sequences). All demappers are based on auxiliary channels of corresponding dimensionality with CS statistics according to (1).

Fig. 1(c) shows the Kullback–Leibler (KL) divergence of 1D and 2D PMFs in relation to the 4D PMF as a function of shaping length. The divergence reduces with shaping length, i.e., it is significant at short shaping length and converges at longer lengths. The performance in terms of AIR and corresponding penalties in relation to the 4D case can be seen in Fig. 1(a) and (b), where considerable AIR penalty is observed only at shorter shaping lengths, while for longer lengths the penalty is negligible.

Auxiliary Channel Dimensionality: Further, we investigate the impact of using different soft-demappers in terms of dimensionality and noise statistics in an experimental nonlinear fiber channel, as shown in Fig. 2. The experimental data are obtained in an extended-reach single-span link[9], where 9 channels at 56 GBd were propagated over 200 km of standard single-mode fiber; the signaling scheme is HCSS with shaping rate of 1.75 b/Amp and 4D symbol mapping based on DP-64QAM. We consider a 1D AC-CS demapper (1D centroids), 2D AC-VPD and SC-CG demappers (2D centroids), and 4D AC-VPD and SC-CG demappers (4D centroids). Since a mismatched PMF does not introduce considerable penalty, we fixed the PMF for all demappers to be the 1D PMF (2D and 4D PMFs are the products of 1D PMF).

Figs. 3(a) and (b) show AIR as functions of

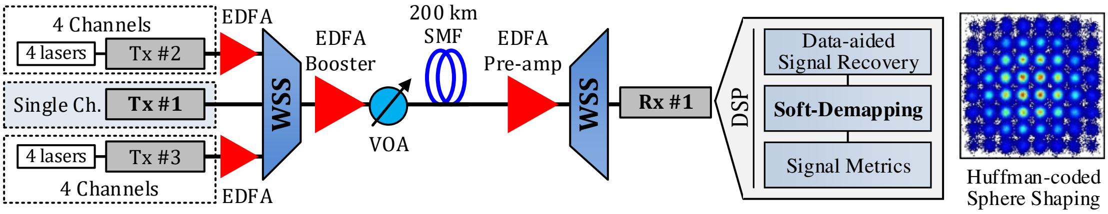

Fig. 2: Experimental setup for 200 km single-span transmission[9].

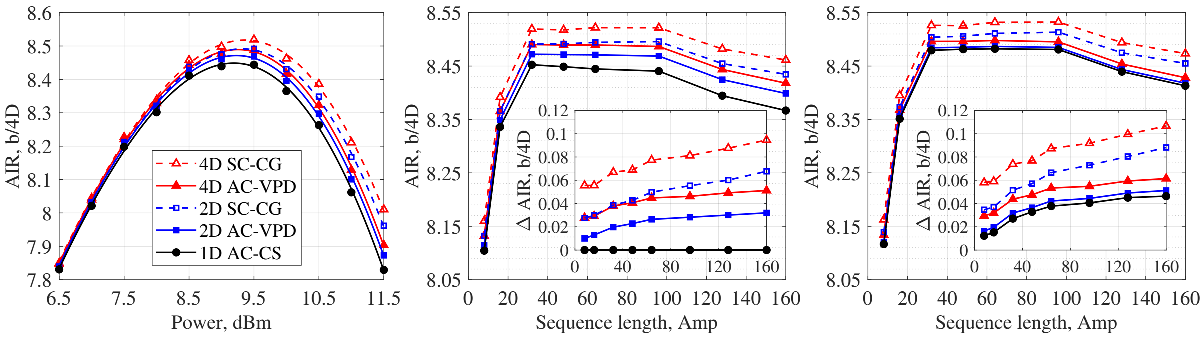

(a) AIR vs. launch power (w/o NLin comp) **(b)** AIR at optimal power w/o NLin comp **(c)** AIR at optimal power w/ NLin comp

Fig. 3: Impact of dimensionality of auxiliary channels. (b)-(c) insets: AIR gain wrt. 1D demapper w/o NLin comp.

launch power (for a shaping length of $L = 48$) and shaping length (at an optimal launch power), respectively. In Fig. 3(a) individual data points represent measured experimental data, and smooth lines represent the data fit, while in Fig. 3(b) AIRs at optimal launch powers are based on the fitted data. Fig. 3(a) shows that the 2D and 4D demappers can achieve substantial gain over the 1D demapper in the nonlinear regime; for $L = 48$, the 2D AC-VPD demapper provides AIR gain of 0.025 b/4D and an additional 0.02 b/4D with CG statistics, while the 4D AC-VPD demapper gives 0.045 b/4D gain and an extra 0.03 b/4D gain with CG statistics. The gain is higher in the highly nonlinear regime, while in the linear regime it becomes negligible, implying that the impact of transceiver imperfections is negligible in our system. Also, from Fig. 3(b) we observe that the gain from 2D/4D demappers is decreased at shorter shaping length (i.e., for the 4D SC-CG demapper and $L = 8$, the gain is 0.055 b/4D, while for $L = 160$, the gain is 0.1 b/4D), which can be explained by the overall increased nonlinear tolerance of short-length shaping[9].

Instantaneous Nonlinearity Compensation

To mitigate the impact of nonlinearities, we use intensity dependent instantaneous nonlinearity compensation, as follows: $E'_* = E_* \exp(-i\alpha P)$, where $P = |E_x|^2 + |E_y|^2$, E_* is the optical field at x/y-polarizations and α is the nonlinear parameter to be optimized at every launch power and shaping length. Fig. 3(c) shows the performance in terms of AIR of the soft-demappers after nonlinearity compensation. Substantial gains are observed, especially, for the 1D AC-VPD demapper. The impact of varying centroid dimensionality is significantly reduced, i.e., at $L = 48$ for the 1D demapper the AIR is improved by 0.035 b/4D and the difference to the 2D AC-VPD demapper becomes negligible, while the 4D VPD demapper provides only a small gain of 0.015 b/4D. Nevertheless, the use of CG statistics provides considerable gain. We note due to more significant nonlinear distortions at longer shaping lengths, the gain from nonlinearity compensation is higher (0.045 b/4D at $L = 160$ for the 1D demapper).

Discussion and Conclusions

We have analyzed various mismatched soft-demappers for systems suffering from strongly correlated nonlinearity. A mismatched PMF for probabilistic shaping with 4D symbol mapping has negligible impact at practical shaping lengths, allowing a low-complexity 1D demapper. However, in the presence of strongly correlated nonlinearity, increasing the dimension of the demapper auxiliary channel provides significant gain by considering the centroids deviations and advanced symbol-wise noise statistics. Alternately, low-complexity nonlinearity compensation can be used to mitigate the centroid deviations, and significantly improve the performance of a 1D demapper.

References

[1] G. Bocherer, F. Steiner, and P. Schulte, “Bandwidth efficient and rate-matched low-density parity-check coded

modulation", *IEEE Transactions on Communications*, vol. 63, no. 12, pp. 4651–4665, 2015.

[2] J. Cho, X. Chen, S. Chandrasekhar, G. Raybon, R. Dar, L. Schmalen, E. Burrows, A. Adamiecki, S. Corteselli, Y. Pan, D. Correa, B. McKay, S. Zsigmond, P. Winzer, and S. Grubb, "Trans-atlantic field trial using probabilistically shaped 64-QAM at high spectral efficiencies and single-carrier real-time 250-Gb/s 16-QAM", in *Proceedings of Optical Fiber Communications Conference (OFC)*, 2017.

[3] H. Sun, M. Torbatian, M. Karimi, R. Maher, S. Thomson, M. Tehrani, Y. Gao, A. Kumpera, G. Soliman, A. Kakkar, M. Osman, Z. A. El-Sahn, C. Doggart, W. Hou, S. Sutarwala, Y. Wu, M. R. Chitgarha, V. Lal, H. Tsai, S. Corzine, J. Zhang, J. Osenbach, S. Buggaveeti, Z. Morbi, M. I. Olmedo, I. Leung, X. Xu, P. Samra, V. Dominic, S. Sanders, M. Ziari, A. Napoli, B. Spinnler, K. Wu, and P. Kandappan, "800G DSP ASIC design using probabilistic shaping and digital sub-carrier multiplexing", *IEEE/OSA Journal of Lightwave Technology*, vol. 38, no. 17, pp. 4744–4756, 2020.

[4] Z. Qu and I. B. Djordjevic, "On the probabilistic shaping and geometric shaping in optical communication systems", *IEEE Access*, vol. 7, pp. 21 454–21 464, 2019.

[5] A. Amari, S. Goossens, Y. C. Gültekin, O. Vassilieva, I. Kim, T. Ikeuchi, C. M. Okonkwo, F. M. J. Willems, and A. Alvarado, "Introducing enumerative sphere shaping for optical communication systems with short blocklengths", *IEEE/OSA Journal of Lightwave Technology*, vol. 37, no. 23, pp. 5926–5936, 2019.

[6] T. Fehenberger, D. S. Millar, T. Koike-Akino, K. Kojima, K. Parsons, and H. Griesser, "Analysis of nonlinear fiber interactions for finite-length constant-composition sequences", *IEEE/OSA Journal of Lightwave Technology*, vol. 38, no. 2, pp. 457–465, 2020.

[7] O. Geller, R. Dar, M. Feder, and M. Shtaif, "A shaping algorithm for mitigating inter-channel nonlinear phase-noise in nonlinear fiber systems", *IEEE/OSA Journal of Lightwave Technology*, vol. 34, no. 16, pp. 3884–3889, 2016.

[8] P. Skvortcov, I. Phillips, W. Forysiak, T. Koike-Akino, K. Kojima, K. Parsons, and D. S. Millar, "Nonlinearity tolerant LUT-based probabilistic shaping for extended-reach single-span links", *IEEE Photonics Technology Letters*, vol. 32, no. 16, pp. 967–970, 2020.

[9] P. Skvortcov, I. Phillips, W. Forysiak, T. Koike-Akino, K. Kojima, K. Parsons, and D. S. Millar, "Huffman-coded sphere shaping for extended-reach single-span links", *IEEE Journal of Selected Topics in Quantum Electronics*, vol. 27, no. 3, pp. 1–15, 2021.

[10] A. Alvarado and E. Agrell, "Four-dimensional coded modulation with bit-wise decoders for future optical communications", *IEEE/OSA Journal of Lightwave Technology*, vol. 33, no. 10, pp. 1993–2003, 2015.

[11] T. A. Eriksson, T. Fehenberger, P. A. Andrekson, M. Karlsson, N. Hanik, and E. Agrell, "Impact of 4d channel distribution on the achievable rates in coherent optical communication experiments", *IEEE/OSA Journal of Lightwave Technology*, vol. 34, no. 9, pp. 2256–2266, 2016.

[12] T. Fehenberger, T. A. Eriksson, A. Alvarado, M. Karlsson, E. Agrell, and N. Hanik, "Improved achievable information rates by optimized four-dimensional demappers in optical transmission experiments", in *Proceedings of Optical Fiber Communications Conference (OFC)*, 2016.